

Supplementary Information

Profiling the evanescent field of nanofiber waveguides using self-assembled polymer coatings

Ilsun Yoon,^a Sarah E. Baker,^b Kanguk Kim,^a Yinmin Wang,^b Sadik C. Esener,^{ac} and Donald J.

*Sirbuly^{*a}*

^aDepartment of NanoEngineering, University of California, San Diego, La Jolla, CA 92093, USA

^bPhysical and Life Sciences Directorate, Lawrence Livermore National Laboratory, Livermore, CA 94550, USA

^cDepartment of Electrical and Computer Engineering, University of California, San Diego, La Jolla, CA 92093, USA

* email: dsirbuly@ucsd.edu

- 1. Experimental procedures**
- 2. Thickness calibration of the PEM coatings using TEM and ellipsometry analysis**
- 3. Fluorescence of FITC with PEM coatings on the WG**
- 4. Power dependent fluorescence of FITC**
- 5. FDTD study of the evanescent field distribution of a WG in mediums with different indices of refraction (from $n = 1$ to $n = 1.45$)**
- 6. Intermittent fluorescence of CdSe Qdots in the evanescent field**

1. Experimental procedures

SnO₂ nanofiber synthesis: SnO₂ nanofibers were synthesized by thermally vaporizing SnO powders in the presence of trace amounts of O₂, similar to previous methods.¹⁻² An alumina boat filled with SnO powder was heated (~1100 °C) in an alumina tube furnace, under 25 sccm flow of Ar at 300 Torr for ~1 hour. After growth the free-standing nanofibers were transferred from the alumina boat surface to a 400 nm SiO₂ coated Si substrate. The nanofibers were manipulated and/or transferred to secondary substrates (e.g., SiO₂ trenches or microfluidic devices) using a 3-dimensional micromanipulator equipped with a tungsten probe.

Optical microscopy. Optical characterization of the nanofiber WGs was performed on a dark-field optical microscope equipped with a 50× (Nikon, NA 0.55) objective, EMCCD camera (Andor Technology), and a fiber coupled spectrometer (Princeton Instruments). WGs were excited by the 442 nm line of a horizontally polarized continuous-wave helium cadmium laser (Kimmon electric). The beam was focused onto the WG with an ~50 μm spot size at an angle of ~45° relative to the sample plane. Power density of the focused 442 nm spot was ~3 W/cm². The microscope was also equipped with a 440 nm band pass excitation filter (fwhm = 10 nm) and 460 nm long pass filter to carry out epi-fluorescence measurements using the tungsten-halogen illumination source.

Fluorescence-based near-field profiling. Nanofibers were suspended over a SiO₂ microchannel (50 μm wide x 4 μm deep) using a 3-axis micromanipulator (World Precision Instruments) to produce free standing optical fibers. Both ends of the WG were clamped on the substrate with polydimethylsiloxane (PDMS). One of the end facets of the fiber was left exposed to air to allow 442 nm light to be launched into the WG. The WGs were precleaned with diluted piranha (H₂SO₄:H₂O₂ = 3:1), RCA solutions (H₂O/H₂O₂/NH₄OH = 5:1:1) and deionized (DI) water (>18.0 MΩ) before polyelectrolyte polymers were deposited on the WG surface. The polyelectrolyte polymers, used for controlling the gap separation between the WG and fluorescent dye, were all purchased from Aldrich. Poly(ethylenimine) (PEI, 750,000 g/mol) was used as the priming layer on the WG. Poly(allylamine hydrochloride) (PAH, 56,000 g/mol) and poly(sodium 4-styrene sulfonate) (PSS, 70,000 g/mol) were used as the alternating polycation and polyanion, respectively. PAH tagged with fluorescein isothiocyanate (FITC) (PAH-FITC, 56,000 g/mol) was used as the final fluorescent layer. The fluorescence intensity generated by the evanescent field or epi-illumination was captured using the EMCCD. The number of alternating PAH and PSS layers was incrementally changed to profile the near-field as a function of separation. After each measurement the polyelectrolyte films were removed by focusing the 325 nm UV light on the WG to decompose the polyelectrolyte followed by a 3h soak in a diluted piranha solution.

The fluorescence data was corrected for quenching and surface area effects by performing epi-fluorescence measurements alongside the evanescent field experiments. As described in the equations below, the fluorescence signal from the chromophores in the evanescent field is proportional to the product of the evanescent field intensity, the number of fluorescing chromophores, and fluorescence efficiency of the chromophores. Similarly, the epi-fluorescence signal taken from far-field excitation of the chromophores is proportional to the product of the epi excitation power, number of fluorescing chromophores, and fluorescence efficiency of the chromophores. With a constant epi-illumination power, dividing the evanescent fluorescence signals (Fig. 2c) by the epi-fluorescence signals (Fig. 2d) from the same samples, the relative evanescent field intensity can be profiled as a function of the distance from the nanofiber surface (red trace, Fig. 3a).

$$\begin{aligned} \text{Normalized Intensity} &= \frac{\text{Evanescent Fluorescence Intensity}}{\text{epi Fluorescence Intensity}} \\ &\propto \frac{e \cdot n \cdot f(d)}{e \cdot n \cdot p} \\ &\propto f(d) \end{aligned}$$

where e is the fluorescence efficiency of the chromophores, n is the number of chromophores, $f(d)$ is the evanescent field intensity as function of the distance (d), and p is the epi-illumination power which was held constant. Since we are only interested in the relative change in $|E|^2$ as a function of distance, and we are simultaneously measuring the extent of quenching through epi-fluorescence, this strategy should be able to correct for the field intensity on any substrate.

FDTD simulations. Guided modes (first and second order lowest modes) on a 200×200 nm SnO₂ WG ($n = 2.1$) at $\lambda = 442$ nm in air were computed using the finite element method (RSoft FemSIM) and launched down the WG. The electric field near the WG surface was mapped out from the power (time-averaged Poynting vector) distribution calculation using the three-dimensional finite-difference time-domain (FDTD) method (RSoft FullWAVE). Additional information on the guided modes in the SnO₂ nanofiber waveguides can be found elsewhere.³

2. Thickness calibration of the PEM coatings using TEM and ellipsometry analysis

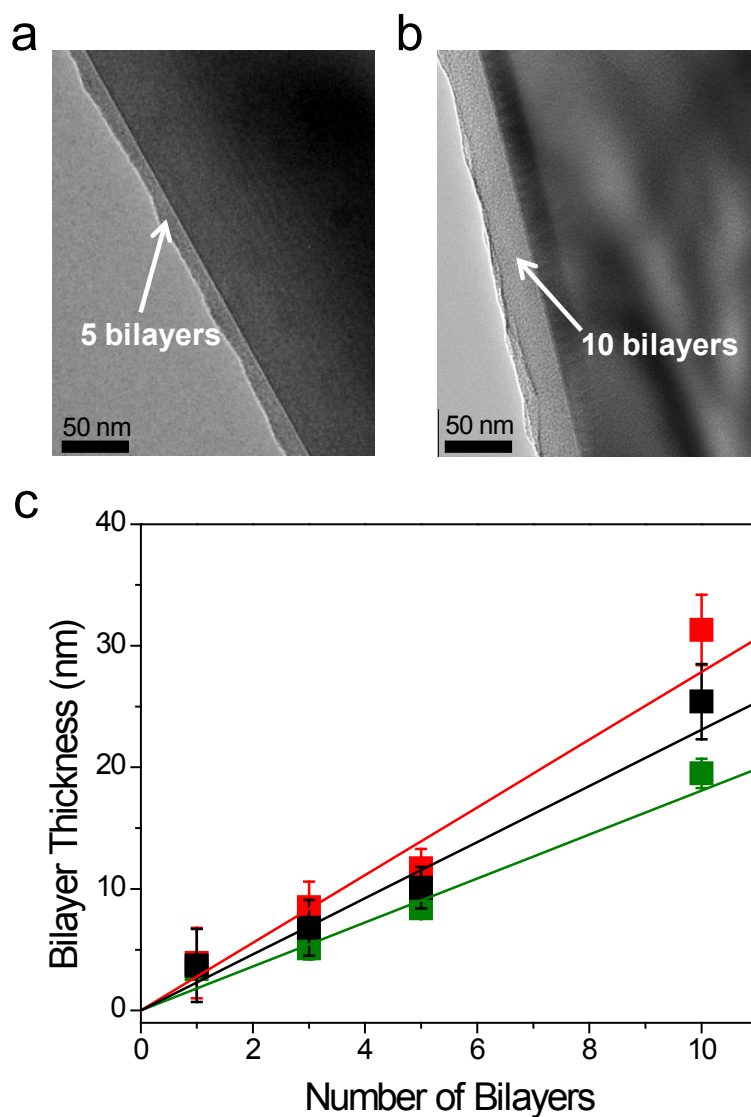


Fig. S1 TEM images showing (a) 5 bilayer and (b) 10 bilayer polyelectrolyte multilayer (PEM) coatings on SnO₂ WGs. (c) Polyelectrolyte thickness (black), determined by averaging thickness values estimated from TEM (red) and ellipsometry analysis (green), as a function of the number of bilayers. For the ellipsometry measurement, PEM coatings of different thickness were prepared on Si substrates. For the TEM measurement, PEM coatings with different thicknesses were prepared on SnO₂ WGs prelocated over TEM grids. Poly(ethylenimine) (PEI) was used as the priming layer on the substrate and WG. Poly(allylamine hydrochloride) (PAH) and poly(sodium 4-styrene sulfonate) (PSS) were used as the alternating polycation and polyanion, respectively. The average slope of the data is 2.3 nm per bilayer.

3. Fluorescence of FITC with PEM coatings on the WG

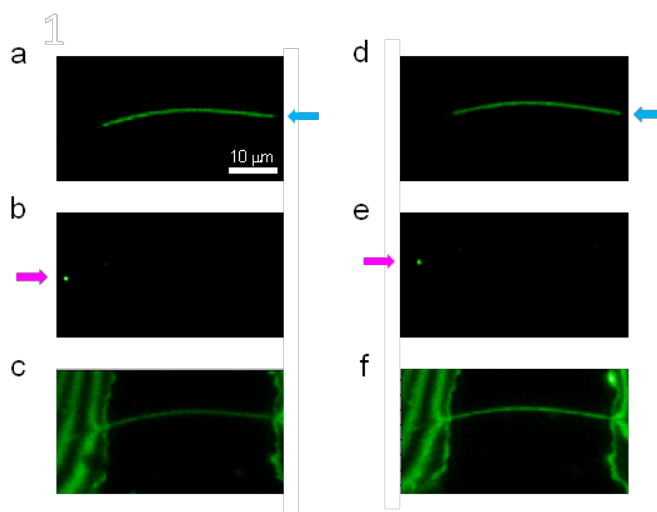


Fig. S2 (a) Evanescent fluorescence image of a WG coated with 1 PE bilayer. The fluorescence is generated with the evanescent field after pumping the WG with the 442 nm light. Cyan arrows indicate the propagation direction of the guided 442 nm light. (b) Scattered emission of the guided 442 nm light at the end-facet of the WG (magenta arrow). Approximately 10% of the total emitted light at the end-facet of the WG is collected via the objective (N.A.: 0.55, solid angle: $\sim 0.3 \pi$).⁴ The fluorescence intensity of (a) is divided by the scattering emission of (b) to normalize with the excitation laser power. (c) Epi-fluorescence image of the WG. Normalized evanescent fluorescence signals are divided by the epi-fluorescence signal to correct for the fluorescence quenching and total number of FITC molecules near the SnO₂ WG surface. (d) Evanescent fluorescence image, (e) scattered emission at the end-facet of the WG, and (f) epi-fluorescence image of the WG coated with 5 PE bilayers.

4. Power dependent fluorescence of FITC

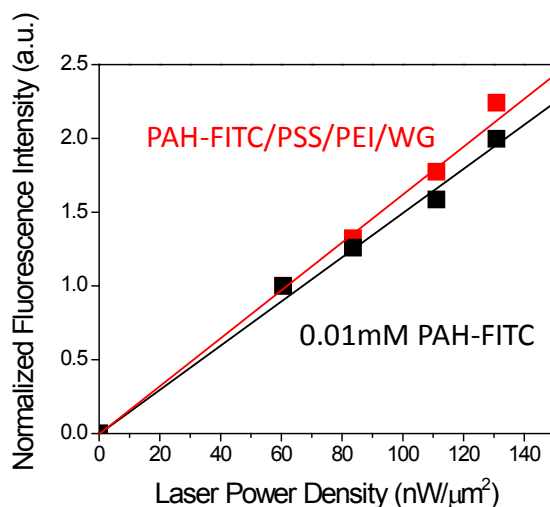


Fig. S3 Plot showing fluorescence from a WG coated with PAH-FITC/PSS/PEI bilayers (red) and a 0.01 mM PAH-FITC solution drop (black) as a function of laser power. At the laser powers used in the WG experiments, no non-linear effects were observed.

5. FDTD study of the evanescent field distribution of a WG in mediums with different indices of refraction (from $n=1.00$ to $n=1.45$)

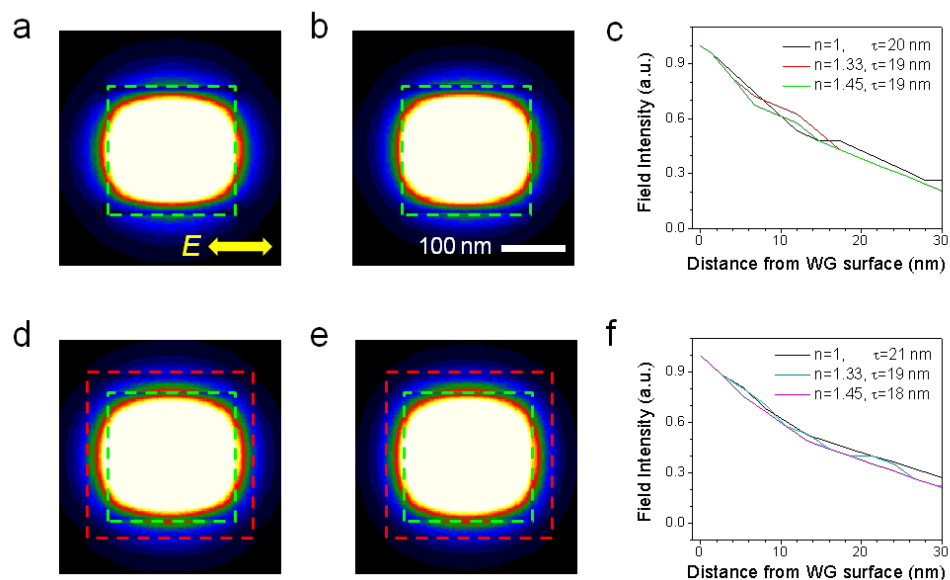


Fig. S4 Evanescent field power distributions (time-averaged Poynting vector) of a WG in mediums with (a) $n = 1.00$ and (b) $n = 1.45$. The polarization of the guided light is horizontal (yellow arrow). Green dash boxes outline the actual WG cavity (200 x 200 nm). (c) Evanescent field profiles near the WG surface at different indices of refraction: $n = 1.00$ (black), $n = 1.33$ (red), and $n = 1.45$ (green). Each decay is fit with a single exponential giving decay constants of 20 nm (black) and 19 nm (red, green). (d-e) Evanescent field distribution of a WG coated with a 30 nm PEM ($n = 1.45$) in a medium with (d) $n = 1.00$ and (e) $n = 1.45$. Red dashed boxes outline the polyelectrolyte layer on the WG. (f) Evanescent field profiles near the surface of the 30 nm PEM-coated WG in mediums with $n = 1.00$ (black), $n = 1.33$ (cyan), and $n = 1.45$ (magenta). Each decay is fit with a single exponential giving decay constants of 21 nm (black), 19 nm (cyan), and 18 nm (magenta). The FDTD simulations show that the field distribution of a WG with a large index ($n = 2.1$) is not significantly affected by a cladding layer of 30 nm thickness. Only small changes (≤ 1 nm) in the decay constants of (c) and (f) are observed when the refractive index of the cladding is changed from 1.33 to 1.45.

6. Intermittent fluorescence of CdSe Qdots in the evanescent field

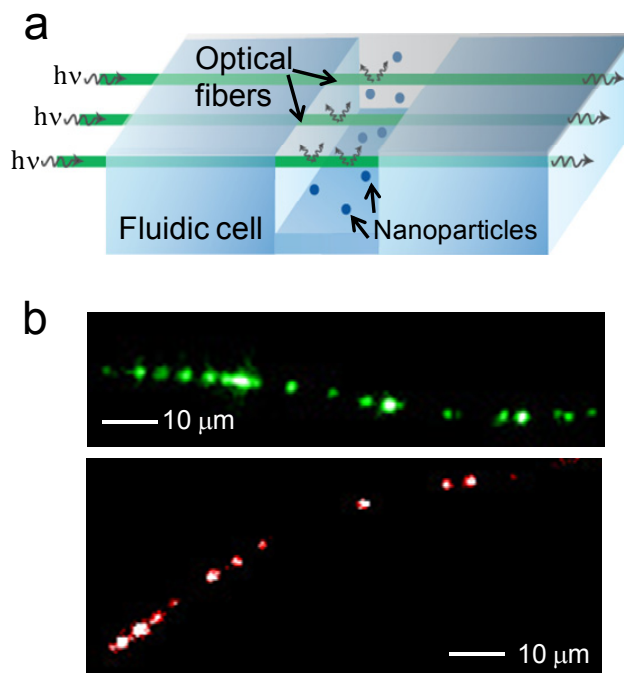


Fig. S5 (a) Schematic of a microfluidic chip with integrated nanofiber WGs traversing across a channel. (b) Optical images (false color) of individual 80 nm gold (*top*) and 10 nm CdSe (*bottom*) nanoparticles bound to a SnO_2 nanofiber WG. Both can act as excellent optical transmitters and provide sensitive feedback on their distance from the WG surface, but the fluorescent nanoparticles can show intermittent emission (i.e., blinking) which can make it more difficult to correlate intensity signals with distance (see Fig. S6). The nanoparticles are being excited with the evanescent field which generates plasmonic scattering and fluorescence signals from the gold and CdSe nanoparticles, respectively. The WGs were embedded in a microfluidic channel so only a portion of their cavities were exposed to the optical transmitters.

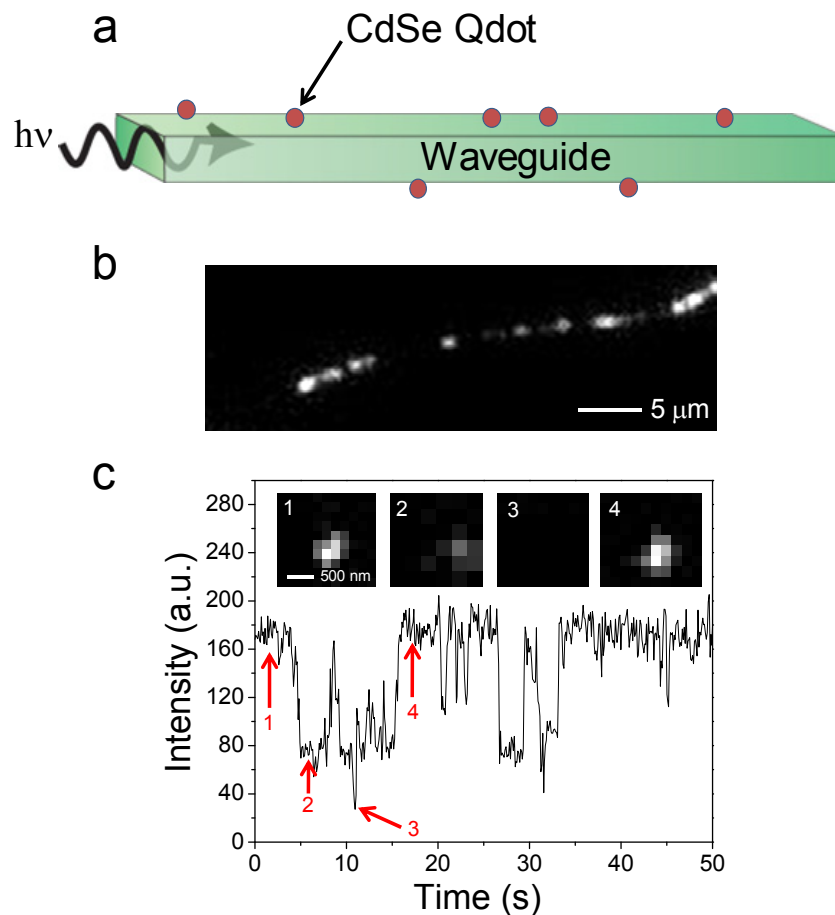


Fig. S6 (a) Schematic showing individual CdSe quantum dots (QDs) decorating the surface of a SnO₂ WG. (b) Optical image of 10 nm CdSe quantum dots fluorescing in the evanescent field of a SnO₂ nanofiber WG. The QDs were coated with streptavidin and the WGs were functionalized with a biotinylated 1,2-dioleoyl-*sn*-glycero-3-phosphocholine (DOPC) lipid bilayer to induce binding. (c) Intensity time course of an individual quantum dot showing intermittent fluorescent behavior while being excited by the near-field of the nanofiber. (*inset*) Fluorescent images of the QD at designated points during the time course. The blinking dynamics of semiconductor quantum dots make them difficult to use as optical transmitters.

Notes and references

- 1 Z. W. Pan, Z. R. Dai and Z. L. Wang, *Science*, 2001, **291**, 1947-1949.
- 2 D. J. Sirbuly, M. Law, J. C. Johnson, J. Goldberger, R. J. Saykally and P. D. Yang, *Science*, 2004, **305**, 1269-1273.
- 3 Z. Ye, X. H. Hu, M. Li, K. M. Ho, and P. Yang, *Appl. Phys. Lett.*, 2006, **89**, 241108.
- 4 I. Yoon, K. Kim, S. E. Baker, D. Heineck, S. C. Esener and D. J. Sirbuly, *Nano Lett.*, 2012, **12**, 1905-1911.